Chiral Discrimination in Solutions and in Langmuir Monolayers

David Andelman[*,†] **and Henri Orland**[‡,§]

Contribution from the School of Physics and Astronomy, Raymond and Beverly Sackler Faculty of Exact Sciences, Tel Aviv University, Ramat Aviv 69978, Tel Aviv, Israel, Service de Physique Théorique, CE-Saclay, F-91191 Gif-sur-Yvette Cedex, France, and Groupe de Physique Statistique, Université de Cergy-Pontoise, BP 8428, 95806 Cergy-Pontoise Cedex, France

Received July 12, 1993[⊗]

Abstract: In this paper we examine theoretically the chiral discrimination of molecules with a single chiral center. We propose a definition of the chiral discrimination parameter Δ in terms of the difference between the second virial coefficient of pure enantiomers and their racemic mixture. This parameter enters in the equation of state of racemic mixtures and will determine their phase diagrams. We calculate then the chiral discrimination between D- and L-alanine using a Monte Carlo simulation to average over 11 molecular degrees of freedom at fixed intermolecular distances using the CHARMM energy function. The discrimination is found to slightly favor homochirality and mainly comes from steric hindrance at short distances. We also perform a direct integration for rigid chiral tetrahedron-shaped molecules. Here there are only five rotational degrees of freedom. For a Lennard–Jones potential, the overall chiral discrimination is found to be predominantly heterochiral. One of our main observations is that the pair free energy, internal energy, and entropy differences between the two enantiomers may change signs as a function of the interpair distance. We find that homochirality is preferred at shorter distances whereas heterochirality is favored at larger distances. With our model molecules a strong chiral discrimination of about 43% is found. The calculation is repeated for molecules that are restricted to lie at the water/air interface. Those model molecules can be regarded as *tripodal* amphiphiles creating a *chiral* Langmuir monolayer at the water/air interface. Here the chiral discrimination is found to be smaller (about 8.8%) but still significantly heterochiral.

I. Introduction

Although the concept of chirality in organic molecules such as proteins, sugars, lipids, etc. was recognized by Pasteur,[1] Le Bel,[2] and van't Hoff[3] over a century ago as a consequence of the asymmetrical nature of tetravalent carbon, it still remains a fascinating area of current research.[4–9] One of the simplest chiral molecules which can be considered is a carbon sitting at the origin of a tetrahedron and covalently connected to four *different* groups. Two distinct stereomers can be formed by reordering the four groups. Those are the two *enantiomers*, D and L, of the chiral molecule, and as can be seen in Figure 1, one is the mirror image of the other.

Although chirality has such a fundamental importance in organic chemistry and biology, its origin is far from being well understood. Practically, it is of great importance to understand what causes some *enantiomeric* liquid mixtures to crystallize as *conglomerates* (*i.e.*, a mixture of crystals of the two pure enantiomers), while others as *racemic compounds* (called sometimes "true racemates") which are true homogeneous crystals of the two enantiomers.[4,9] On a microscopic level, one can distinguish between two cases. In the first, the interaction between a pair of the same enantiomers, D–D (or L–L), is more preferable than that of the mixed pair, D–L. This preference is called *homochirality*. In the second case, the preference is for the D–L pair and is called *heterochirality*. The difference in the interaction energies of the D–D (or L–L) and D–L pairs known as the *chiral discrimination* is the main factor determining how a liquid *racemic* mixture of D and L will crystallize.

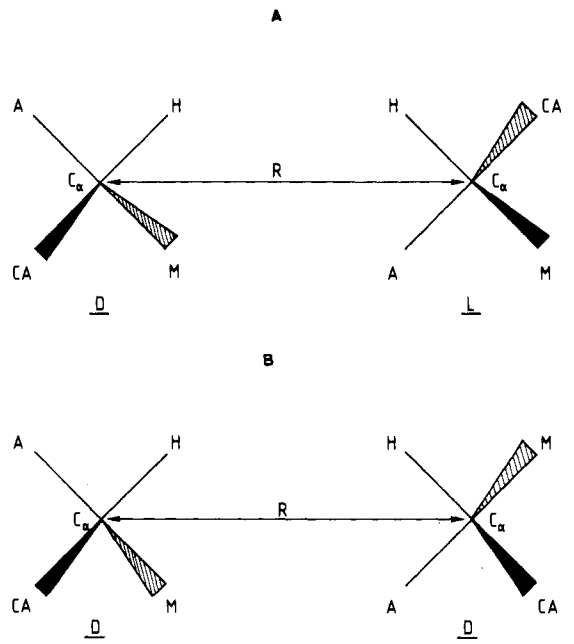

Figure 1. Simple molecule with a single chiral center represented as a tetrahedron. Four groups, A, M, CA, and H, are connected to the chiral center at the origin C_α. The two chiralities are denoted by D and L. In A we show the D–L pair at a distance R, and in B the D–D pair.

† Tel Aviv University.
‡ Service de Physique Théorique.
§ Université de Cergy-Pontoise.
⊗ Abstract published in *Advance ACS Abstracts*, November 1, 1993.

(1) Pasteur, L. *Ann. Chim. Phys.* **1848**, *24*, 442.
(2) Le Bel, J. A. *Bull. Soc. Chim. Fr.* **1874**, *22*, 337.
(3) van't Hoff, J. H. *Arch. Neerl. Sci. Exactes Nat.* **1874**, *9*, 445.
(4) *Optical Activity and Chiral Discrimination*; Mason, S. F., Ed.; Reidel: Dordrecht, The Netherlands, 1979.
(5) Mason, S. F. *Chemical Evolution*; Clarendon Press: Oxford, U.K., 1991; Chapter 14.
(6) Maddox, J. *Nature* **1989**, *341*, 101.
(7) Craig, D. P.; Mellor, D. P. *Top. Curr. Chem.* **1976**, *63*, 1.
(8) Kagan, H. *C. R. Acad. Sci.*, Ser. Gen.: Vie Sci. **1985**, *2*, 141.
(9) For a detailed review on racemic mixtures, see: Jacques, J.; Collet, A.; Wilen, S. H. *Enantiomers, Racemates and Resolutions*; Wiley: New York, 1981 and references therein.

0002-7863/93/1515-12322$04.00/0 © 1993 American Chemical Society

Several attempts have been made to study the discriminating forces between chiral molecules. For instance, Craig,[10] Schipper,[11] and co-workers used multipole expansions and found a very rapid decay of the chiral forces for quadrupoles and higher multipoles. Both pure electrostatic and dispersion (van der Waals) forces have been investigated.

A different approach was used by Salem *et al.*[12] Interaction energies were calculated between two model chiral tetrahedra. In the freely rotating limit (infinite temperature) they showed that chiral discrimination cannot exist if only two-body interactions are considered. Weak discrimination was found using six-body or higher order interactions. At finite temperatures (using Boltzmann weighted averaging) and for pure electrostatic interactions, they found a very small discrimination. However, their numerical procedure did not converge well for the shorter intermolecular distances where the discrimination is more significant.

In a different work,[13,14] significant chiral discrimination was found for *tripodal*-shaped molecules which can be thought of as a model for amphiphiles creating a chiral Langmuir monolayer. There, Boltzmann weighted averaging at finite temperatures yielded a discrimination for various types of two-body interactions: van der Waals, charges, and dipoles. One of the striking results obtained is that van der Waals interactions between tripodal molecules tend to favor heterochirality whereas, in some cases, electrostatic interactions favor homochirality. However, this particular model averages only over nine discrete back-to-back intermolecular rotations instead of doing the full integration over the angular-phase space.

The aim of the present work is to elucidate even further the origin of chiral discrimination. In section II, we conveniently define the chiral discrimination parameter and its connection to molecular interactions and thermodynamics of racemic mixtures. In view of recent success in simulating complex molecules using standard two-body force fields[15-18] like CHARMM, AMBER, and OPLS, we have calculated the chiral discrimination between L- and D-alanine (section III) using Monte Carlo simulation. However, due to ever-present stochastic errors even in very large computer runs and the small discrimination in alanine, we have also performed numerical integrations over the rotational degrees of freedom (with the correct Boltzmann weight at finite temperature) on *model* molecules interacting via a two-body Lennard–Jones potential. In section IV, we present results for tetrahedral model molecules in solution (three-dimensional system), and in section V, we repeat the calculations for the same molecules but with an additional constraint that three molecular groups are restricted to lie on a plane. This system can be thought of as a model for a chiral Langmuir monolayer. In both two and three dimensions, a substantial chiral discrimination was obtained. Finally, some concluding remarks are presented in section VI.

II. Chiral Discrimination and Thermodynamics of Racemic Mixtures

Consider a system of N molecules, each consisting of n atoms. By denoting $\vec{R}_i$ the distance to the center of mass of the ith molecule and $\vec{r}_j^{\,i}$ the relative distance of the jth atom of the ith molecule from its center of mass $\vec{R}_i$, the partition function Z of the system reads

$$Z = \int \prod_{i=1}^{N} \mathrm{d}\vec{R}_i \prod_{j=1}^{n} \mathrm{d}\vec{r}_j^{\,i} \prod_{i=1}^{N} \delta\Big(\sum_{j=1}^{n} \vec{r}_j^{\,i}\Big) \exp\Big[-\beta \sum_{i=1}^{N} \sum_{1\le k<l\le n} v_{kl}(\vec{r}_k^{\,i} - \vec{r}_l^{\,i}) - \beta \sum_{1\le i<j\le N} \sum_{k=1}^{n} \sum_{l=1}^{n} v_{kl}(\vec{R}_i - \vec{R}_j + \vec{r}_k^{\,i} - r_l^{\,j})\Big] \quad (1)$$

where $\beta = 1/k_B T$, T is the temperature, and k_B is the Boltzmann constant. The first (second) term in the exponent denotes intramolecular (intermolecular) interactions. The interaction potential $v_{kl}(\vec{r})$ is the two-body interaction of atom (or group) k with atom (or group) l at a distance r, and the δ functions enforce the constrains that each $\vec{R}_i$ is the center of mass of the ith molecule.

Performing a straightforward virial expansion to second order,[19] the free energy F and pressure P read

$$-\beta F = N \log \Omega + N \log Z_1 + {}^1/_2 N\rho \frac{Z_2}{Z_1^{\,2}}$$

and

$$P = \rho k_B T\left(1 - \frac{\rho}{2}\frac{Z_2}{Z_1^{\,2}}\right) \quad (2)$$

where Ω is the volume of the system and the molecular density $\rho = N/\Omega$. The intramolecular (single molecule) partition function Z_1 and its corresponding free energy f_1 are defined as

$$Z_1 = \Omega^{n-1} \exp(-\beta f_1) = \int \prod_{j=1}^{n} \mathrm{d}\vec{r}_j\, \delta\Big(\sum_{j=1}^{n} \vec{r}_j\Big) \exp\Big[-\beta \sum_{1\le k\le l\le n} v_{kl}(\vec{r}_k - \vec{r}_l)\Big] \quad (3)$$

and are independent of the center of mass position $\vec{R}$. Similarly, the two-molecule partition function Z_2 depends only on the center-to-center intermolecular distance, $\vec{R} = \vec{R}_1 - \vec{R}_2$.

$$Z_2 = \int \mathrm{d}\vec{R} \int \prod_{j=1}^{n} \mathrm{d}\vec{r}_j \prod_{j=1}^{n} \mathrm{d}\vec{r}_j'\, \delta\Big(\sum_{j=1}^{n} \vec{r}_j\Big)\delta\Big(\sum_{j=1}^{n} \vec{r}_j'\Big) \exp\Big(-\beta \sum_{1\le j<k\le n} [v_{jk}(\vec{r}_j - \vec{r}_k) + v_{jk}(\vec{r}_j' - \vec{r}_k')]\Big) \times \Big(\exp\Big[-\beta \sum_{j=1}^{n} \sum_{k=1}^{n} v_{jk}(\vec{r}_j - \vec{R} - \vec{r}_k')\Big] - 1\Big) \quad (4)$$

By denoting the free energy of a pair of molecules at distance $\vec{R}$ as $f_2(R)$, and similarly $U_2(R)$ the internal energy and $S_2(R)$ the entropy, we have

$$f_2(R) = U_2(R) - TS_2(R) \quad (5)$$

and

$$\frac{Z_2}{Z_1^{\,2}} = \int \mathrm{d}\vec{R}\, (\exp[-\beta(f_2(R) - f_2(+\infty))] - 1) \quad (6)$$

where at infinite separation there are no intermolecular contributions to the pair free energy and the only contribution to $f_2(+\infty)$ comes from the two intramolecular ones, $f_2(+\infty) = 2f_1$.

Thus, the virial expansion for the pressure can be rewritten as

$$P = \rho k_B T(1 + B_2(T)\rho + \ldots) \quad (7)$$

where $B_2(T)$ is the second virial coefficient given by eq 6.

(10) (a) Craig, D. P.; Power, E. A.; Thirunamachandran, T. *Proc. R. Soc. London* **1971**, *A322*, 165. (b) Craig, D. P.; Schipper, P. E. *Ibid.* **1975**, *A342*, 19. (c) Craig, D. P.; Radom, L.; Stiles, P. J. *Ibid.* **1975**, *A343*, 11.

(11) (a) Schipper, P. E. *Chem. Phys.* **1977**, *26*, 29. (b) *Ibid.* **1979**, *44*, 261. (c) *Ibid.* **1981**, *57*, 105. (d) Schipper, P. E. *Aust. J. Chem.* **1982**, *35*, 1513.

(12) Salem, L.; Chapuisat, X.; Segal, G.; Hiberty, P. C.; Minot, C.; Leforestier, C.; Sautet, P. *J. Am. Chem. Soc.* **1987**, *109*, 2887.

(13) Andelman, D.; de Gennes, P. G. *C. R. Acad. Sci., Ser. 2* **1988**, *307*, 233.

(14) Andelman, D. *J. Am. Chem. Soc.* **1989**, *111*, 6536.

(15) Brooks, B. R.; Bruccoleri, R. E.; Olafson, B. D.; States, B.; Swaminathan, S.; Karplus, M. *J. Comput. Chem.* **1983**, *4*, 187.

(16) Smith, J. C.; Karplus, M. *J. Am. Chem. Soc.* **1992**, *114*, 801.

(17) Weiner, S. J.; Kollman, P. A.; Case, D. A.; Chandra Singh, U.; Ghio, C.; Alagona, G.; Profeta, S., Jr.; Weiner, P. *J. Am. Chem. Soc.* **1984**, *106*, 765.

(18) Jorgensen, W. L.; Tirado-Rives, J. *J. Am. Chem. Soc.* **1988**, *110*, 1657.

(19) Hansen, J.-P.; McDonald, I. R. *Theory of Simple Liquids*, 2nd ed.; Academic Press: New York, 1986.

$$B_2(T) = -\frac{Z_2}{2Z_1^2} \equiv \frac{1}{2}\int d\vec{R}\, b_2(T,R) \quad (8)$$

The above equation of state can be generalized to a racemic mixture having a molar fraction x of the D enantiomer and $1 - x$ of the L enantiomer.

$$P = \rho k_B T[1 + \rho B_2^{DD} + 2\rho x(1-x)(B_2^{DL} - B_2^{DD}) + ...] \quad (9)$$

where ρ is the total molecular density. All quantities belonging to the pair D–L (heterochiral) are denoted by DL and all those of the homochiral case (the pair D–D) by DD. Note that from symmetry $B_2^{DD} = B_2^{LL}$ and $B_2^{DL} = B_2^{LD}$.

A chiral discrimination parameter, Δ, can be conveniently defined as the relative difference between the two virial coefficients B_2^{DD} and B_2^{DL}

$$\Delta = \frac{B_2^{DL}(T) - B_2^{DD}(T)}{B_2^{DD}(T)} \quad (10)$$

and the equation of state for the mixture reads

$$P = \rho k_B T(1 + \rho B_2^{DD}[1 + 2x(1-x)\Delta] + ...) \quad (11)$$

This single parameter Δ *encapsulates* the difference in interaction for the D and L enantiomers averaged over the intermolecular distances and takes into account the correct Boltzmann weight at temperature T. For example, if P_A is the pressure of the enantiomeric substance and P_R of the racemate ($x = 0.5$) then

$$\frac{P_R - P_A}{\rho k_B T} = \frac{\rho B_2^{DD}}{2}\Delta$$

The above treatment can be generalized to ternary solutions of the D and L enantiomers and a solvent. Then, the difference in pressures in eq 11 translates into a difference in osmotic pressures. As long as the solvent is achiral, it will change the evaluation of both B_2^{DD} and B_2^{DL} in a similar way. Generalizations to chiral solvents[14,20] or to interactions with a chiral substrate[21-23] are also possible.

Note that, in the infinite temperature limit, Δ reduces to zero for any two-body interactions since

$$\Delta = \lim_{T\to\infty} \frac{\int d\vec{R}\,(U_2^{DL}(R) - U_2^{DD}(R))}{\int d\vec{R}\, U_2^{DD}(R)} = 0 \quad (12)$$

This agrees with the observation of Salem *et al.*[12] that only six-body or higher order interactions will give rise to nonzero Δ at the infinite temperature (freely rotating) limit.

With this definition of Δ (keeping in mind that B_2 is negative for attractive interactions like Lennard-Jones potentials), a positive Δ means that heterochiral interactions (HEC) are favored with respect to homochiral ones; $\Delta = 0$ is the case of no discrimination, and $\Delta < 0$ is the preferred homochiral case (HOC). These general considerations are applied in the following sections where Monte Carlo simulations are presented for alanine molecules (section III) and tetrahedral model molecules in sections IV and V.

III. Chiral Discrimination in Alanine

Alanine is the simplest *chiral* amino acid constituting proteins. Its chemical formula is given by

$$NH_3\text{–}HC_\alpha CH_3\text{–}COO$$

where we use the zwitterionic form of the alanine molecule, appropriate to describe alanine molecules in a polar solvent (aqueous solution). The C_α is an asymmetric carbon and occurs in proteins only in the left-handed chirality (L-alanine). However, it is possible to synthesize both enantiomers (L- and D-alanine). Since all covalent bonds and valence angles can be taken (to a good approximation) to be frozen about their average values, the only remaining intramolecular degrees of freedom are the torsional ones. In order to compute the chiral discrimination between the two enantiomers of alanine, we used the CHARMM all-atom energy function:[15-18]

$$E = \sum_{\text{dihedrals}} k_\phi[1 + \cos(n\phi - \delta)] + \sum_{i<j} 4\epsilon_{ij}\left[\left(\frac{\sigma_{ij}}{r_{ij}}\right)^{12} - \left(\frac{\sigma_{ij}}{r_{ij}}\right)^{6}\right] + \sum_{i<j}\frac{332}{\epsilon_r}\frac{q_i q_j}{r_{ij}} \quad (13)$$

where all distances are given in Å, angles in rad, and energies in kcal/mol (at 300 K, $k_B T$ is given by 0.595 kcal/mol). The first sum in eq 13 is over the dihedrals and represents the total torsional energy of the alanine molecule with torsion coefficients k_ϕ, ϕ (the usual dihedral angle), n (the rotation symmetry), and δ (a phase shift).

The second term is a Lennard–Jones potential summed over all nonbonded pairs (i,j) of atoms at distance r_{ij}. It represents both short-distance steric repulsion and large-distance attraction. For each pair (i,j), the two parameters ϵ_{ij} and σ_{ij} characterizing the energy scale and radius of the interaction, respectively, are defined as

$$\epsilon_{ij} = (\epsilon_i \epsilon_j)^{1/2}$$

and

$$\sigma_{ij} = 2^{-1/6}(\sigma_i + \sigma_j) \quad (14)$$

where ϵ_i and σ_i are the conventional 12:6 Lennard–Jones parameters for any of the types of atoms of alanine. The last term is the direct electrostatic interaction, q_i, being the partial charge of the ith atom (in units of electron charge) as defined by CHARMM. The relative dielectric permittivity, ϵ_r, is set to $\epsilon_r = 80$ in the following, assuming that the solvent is water.

The interaction energy (intermolecular) is made up of only the last two terms: Lennard–Jones and electrostatic. The values of the parameters used in the alanine simulation are listed in Table I. Altogether we integrate over 11 degrees of freedom: three

Table I. Partial Charge, q_i, and Lennard–Jones Potential Parameters σ_i and ϵ_i As Given by the CHARMM Potential (Eqs 13 and 14) for an Alanine Molecule[a]

atom	group	q_i[b]	σ_i[c]	ϵ_i[d]
N	NH_3	0.0	1.6	–0.2384
H	NH_3	+0.33	0.6	–0.0498
H	NH_3	+0.33	0.6	–0.0498
H	NH_3	+0.33	0.6	–0.0498
C	C_α	–0.1	1.8	–0.0903
H	H	+0.1	1.47	–0.0045
C	CH_3	–0.3	1.8	–0.0903
H	CH_3	+0.1	1.47	–0.0045
H	CH_3	+0.1	1.47	–0.0045
H	CH_3	+0.1	1.47	–0.0045
C	COO	0.0	1.8	–0.0903
O	COO	–0.5	1.6	–0.6469
O	COO	–0.5	1.6	–0.6469

[a] The first four atoms form the amine (NH_3) group, the next one the asymmetric C_α carbon, then the single H, the four atoms of the methyl group (CH_3), and the three of the carboxylic acid group (COO). [b] Partial charges in units of electron charge. [c] Distances in Å. [d] Energies in kcal/mol.

(20) Schipper, P. E.; Harrowell, P. R. *J. Am. Chem. Soc.* **1983**, *105*, 723.
(21) Lipkowitz, K.; Demeter, D. A.; Zegarra, R.; Larter, R.; Darden, T. *J. Am. Chem. Soc.* **1988**, *110*, 3446.
(22) Joshi, V.; Kotkar, D.; Ghosh, P. K. *J. Am. Chem. Soc.* **1986**, *108*, 4650.
(23) Jug, A. *C. R. Acad. Sci., Ser. 2* **1986**, *303*, 1773.

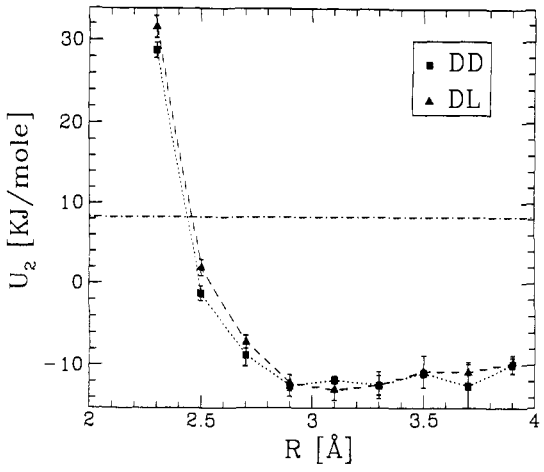

Figure 2. Averaged internal energy U_2 as computed from Monte Carlo simulations of D–D and D–L pairs of alanine molecules as a function of the distance R between the two nitrogens (measured in Å). The D–D data points are represented by the full squares and are connected by a dotted line, whereas those of the D–L data points are represented by full triangles and are connected by a dashed line. The averaging over all allowed configurations is done with the proper Boltzmann weight. All energies are measured in kJ/mol, and the temperature is set to $T = 200$ K. All other parameters are given in Table I. The errors bars are obtained by averaging over five independent runs. The horizontal dotted–dashed line indicates the value of U_2 at infinite separation. A small HOC chiral discrimination can be seen at short distances (≤2.7 Å).

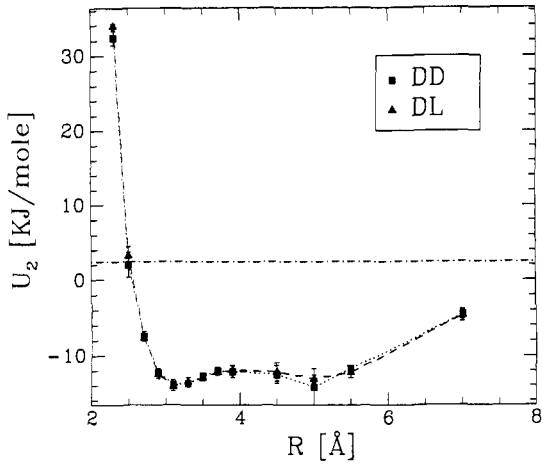

Figure 3. Averaged internal energy U_2 as computed from Monte Carlo simulations of pairs of D–D and D–L alanine molecules. The temperature is set to $T = 300$ K. All other parameters and notations are the same as in Figure 2 (see also Table I). No conclusive chiral discrimination beyond the error bars can be seen at this temperature.

internal rotations for each alanine (accounting for the torsion) and five relative angles for the intermolecular rotations.

The pair partition function, Z_2, defined in eq 4 is used to compute the pair internal energy $U_2(R)$ (eqs 4–6) using the so-called Monte Carlo growth method described in detail in ref 24. The calculations are repeated for the two pairs of alanine, D–D and D–L, as a function of the intermolecular distance R taken to be the distance between the two nitrogens. The distance was varied between 2.3 and 7 Å. In addition, the point of infinite separation was calculated. Five independent runs of 20 000 Boltzmann weighted configurations were generated and used to obtain averages. The Monte Carlo runs have been carried out on a Cray 2 supercomputer. Each independent run took about 10 min of CPU. The total CPU time used to study chiral discrimination in alanine was about 40 h.

The results are shown in Figures 2 and 3 for two temperatures, $T = 200$ and 300 K, respectively. As expected for both D–D and D–L, U_2 has a repulsive core at short distances (≤2.4 Å), followed by a potential well at intermediate distances and an attractive tail at large distances. The point of infinite separation appears as a dotted–dashed line in the figures. Although there is a small chiral discrimination (favoring homochirality), especially at $T = 200$ K and small R, it lies within our stochastic error bars. Our calculations, which give reasonable precision for the individual thermodynamical quantities (free energy, internal energy, and entropy) of each pair, are not precise enough to yield reliable measure of the chiral discrimination. This should not come as a total surprise since the chiral discrimination is expected to be quite small compared with the average quantities.

We have also repeated the Monte Carlo runs for a different form (not zwitterionic) of alanine at $T = 200$ and 300 K. This is the form more appropriate for alanine molecules in the vacuum ($\epsilon_r = 1$) compared to the zwitterionic form which is valid in solution. This form does not have partial charges on the amine and carboxyl groups and is also the form used in simulations of peptides. Although the pair interaction is very different when compared with the zwitterionic case due to a smaller contribution from the electrostatic interactions, the chiral discrimination could not have been resolved here as well. It lies within the stochastic error bars just like in Figures 2 and 3.

We have chosen alanine because it is the simplest chiral amino acid and one of the simpest chiral molecules altogether. However, it seems that the chiral discrimination for alanine is just too small to be measured in computer simulations. Since our simulations were carried out on a large-scale supercomputer and were quite extensive, we do not believe that they can be improved substantially with current state-of-the-art computers. Also, the uncertainities in the definition of the various energy constants in CHARMM can cause large deviations in such small chiral discriminations. It would be interesting to perform similar calculations on different (more complicated) chiral molecules for which the chiral discrimination is known to be sizable.

Another approach which we employed successfully is to try to reduce even further the number of degrees of freedom, the main goal being the feasibility of numerical integration of the two-body partition function, which is impractical even for 11 degrees of freedom of pairs of alanine. In the next sections we describe such a procedure for rigid tetrahedra serving as model chiral molecules.

IV. Chiral Discrimination for Model Molecules

In order to reduce the number of degrees of freedom while preserving the chiral nature of alanine, we replaced each rotating group of the alanine (amine (NH_3), methyl (CH_3), and carboxylic acid (COO)) by a single fictitious spherical particle. The resulting molecule consisted of a C_α carbon sitting in the center of a rigid tetrahedron and four "particles" sitting on the four vertices: particle A representing the amine group, M the methyl, CA the acid group, and H the remaining single hydrogen. Although our starting point is a simplified model for alanine molecules, we model *qualitatively* in this section any chiral molecule with a single chiral center.

Each tetrahedron represents a chiral molecule as long as the four vertices are different one from another (Figure 1). Since it is a rigid body, the only degrees of freedom left are rotations of the entire tetrahedron with respect to its central C_α carbon. As can be seen in Figure 1, there are only two possible isomers, D and L, of the tetrahedron related by permutations of any pair of vertices. Those are the two chiral enantiomers.

Only the last two terms of eq 13 account for the energy function since there is no torsion energy for rigid bodies. Furthermore, for convenience, we set all partial charges, q_i, equal to zero and

(24) (a) Garel, T.; Orland, H. *J. Phys. A* **1990**, *23*, L621. (b) Garel, T.; Niel, J.-C.; Orland, H.; Velikson, B. *J. Chim. Phys. Phys.-Chim. Biol.* **1991**, *88*, 2473.

Table II. Parameters for the Model Tetrahedral Molecules Interacting via Pure Lennard-Jones Potential[a]

group	bond length[b] to C_α	σ[b]	ϵ[c]
C_α	0.0	1.8	−0.1
A	2.25	2.0	−0.35
M	1.5	1.6	−1.5
CA	3.0	3.2	−0.5
H	0.75	0.8	−0.05

[a] The C_α is the central asymmetric carbon. The four groups A, M, CA, and H model the amine, methyl, carboxylic acid, and hydrogen groups of alanine, respectively. They sit at the vertices of the tetrahedron as is illustrated in Figure 1. [b] Distances in Å. [c] Energies in kJ/mol.

leave only the Lennard–Jones interactions. In a more refined calculation, one should include charges and direct dipole–dipole (or higher multipole) interactions since the Lennard–Jones potential accounts only for induced dipoles. Thus, the parameters defining the tetrahedron molecule are the ϵ's and σ's for each one of the five groups (central C_α and the four vertices: A, M, CA, and H). In addition, we need to specify the four rigid bond lengths: C_α–A, C_α–M, C_α–CA, and C_α–H. All these parameters are listed in Table II and completely specify our model molecule. As was mentioned above, the specific values are representative but have been chosen to make the model molecule quite asymmetric and to increase the chiral discrimination. The four valence angles of the central C_α carbon are taken to be equal to the standard value, $\arccos(-1/3) \approx 109.47°$.

At a given intermolecular distance (center-to-center), we calculate the intermolecular interaction energies between the 25 pairs of groups (five on each of the tetrahedra). In order to sum over all possible relative rotations of the D–D and D–L pairs of molecules, we fixed one tetrahedron with a frozen orientation so that its C_α group is at the origin and used five angles to describe the rotational degrees of freedom of the second tetrahedron: three are the Euler angles of rotation of the second tetrahedron about its center (χ_1, χ_2, and χ_3), while the others are the two polar angles θ and ϕ parametrizing the position of the center of the second tetrahedron with respect to the first. The angles θ and χ_2 vary between 0 and π, while all others between 0 and 2π. This procedure ensures that we sum over all relative orientations of the two tetrahedra while keeping their center-to-center distance fixed.

The numerical integration is performed by discretizing the five-dimensional angular space using the Simpson integration method, with $N + 1$ points for θ and χ_2, and $2N + 1$ for χ_1, χ_3, and ϕ. The total number of points for the five-dimensional integration is thus $(2N + 1)^3(N + 1)^2$. Convergence of the integration was checked by calculating the free energy and internal energy, successively, with $N = 8, 10, 12, 14$, and 16. Convergence was better than one part in 10^4 for $N = 16$ (approximately 10^7 points of integration).

In Figure 4 we present $f_2(R)$, $U_2(R)$, and $S_2(R)$ at $T = 300$ K for distances ranging from 2 to 14 Å for both the D–D and D–L pairs. At short distances ($\leq$4 Å) the D–D pair is favored (HOC), whereas at intermediate distances the D–L one is favored (HEC). At large distances ($\geq$10 Å), as expected, they converge to the same value, which is the entropy of rotation: $f_2(\infty) = -TS_2(\infty) = 2f_1$. These results indicate that the steric hindrance favors HOC, whereas HEC is favored energetically at larger distances (in the attractive region of the potential). This is a nontrivial result since it shows that simple-minded models of geometrical packing of D and L molecules are not completely suited to deduce the overall chiral discrimination. Indeed, discrimination in the attractive range of the potential (intermediate distances) may also play a crucial role.

In Figure 5, the integrand of $B_2(T)/2\pi$ (as defined in eq 8), $b_2(T,R)R^2$, is plotted as a function of the inter-pair distance R. The important features of the chiral discrimination at different distances can be seen. At short distances, the large discrimination

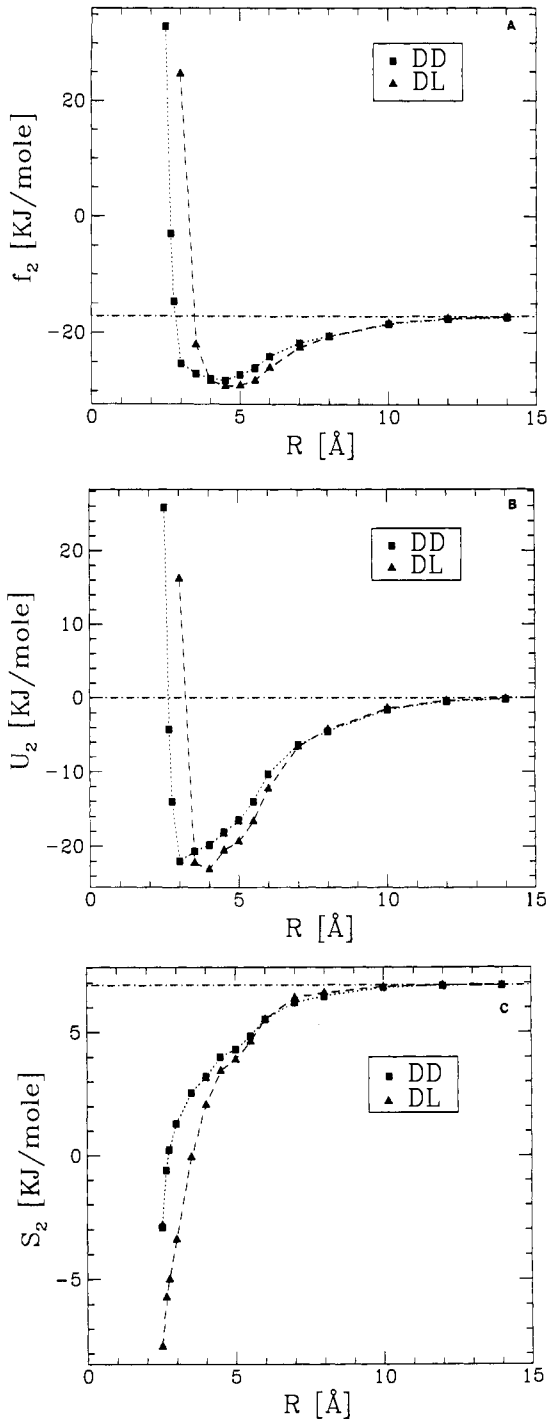

Figure 4. Pair free energy, f_2, internal energy, U_2, and entropy, S_2 (in units of kJ/mol), as functions of the inter-pair distance R (in units of Å) plotted in A, B, and C, respectively. All data points for the D–D pair are marked by full squares, those for the D–L pair by full triangles. The averages are performed using the proper Boltzmann weight and averaging over all possible rotations in three dimensions, while keeping R fixed for each data point. The temperature is set to $T = 300$ K. The values of geometrical and interaction parameters are given in Table II. Note the deeper minima of f_2^{DL} (at $R = 5$ Å) and U_2^{DL} (at $R = 4$ Å) as compared with their D–D counterparts, as well as their steeper rise at short distances due to steric hindrance. The horizontal dotted–dashed lines denote the values at infinite separation.

present in the free energy is strongly suppressed by the exponential weight, whereas in the intermediate range around the potential minimum ($\approx$5 Å), it is significant. The value of the chiral discrimination $\Delta = 0.43$ is obtained by integrating over the intermolecular distance, as is apparent from eq 8. Since $\Delta > 0$, it indicates an overall HEC tendency in our model (with Lennard–

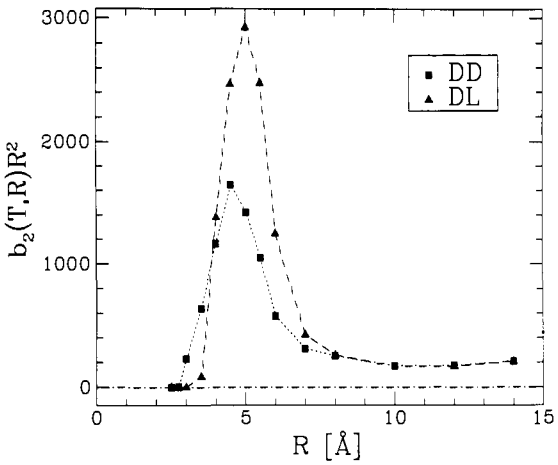

Figure 5. Integrand of the second virial coefficient, $b_2(T,R)R^2$ in 3D, as a function of the inter-pair distance R. Notations are the same as in Figure 4. Note the crossover between a HOC behavior below 4 Å to a HEC one above 4 Å. The difference between the areas under the two curves is proportional to the chiral discrimination parameter Δ. It is clear that HEC is preferred due to the bigger area centered at the (deeper) minimum of the D–L free energy at R = 5 Å.

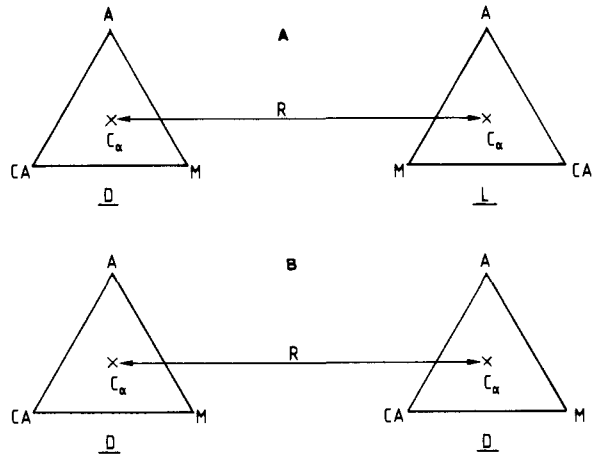

Figure 6. Pair of D–L plotted in A and D–D in B. The three groups are denoted by A, M, and CA. Rotations of the two molecules are restricted to a two-dimensional plane. The two enantiomers, D and L, are related by any pair permutation of the three groups A, M, and CA. This model molecule can be viewed as the basal plane of a *tripodal* chiral molecule where the fourth group points always perpendicular to the plane and does not contribute to the chiral discrimination.

Jones potential), although this tendency is contrary to the HOC behavior at very short distances due to steric hindrance.

Our results should be compared with those of Salem *et al.*[12] In both works, the chiral molecules used are rigid tetrahedra having five degrees of freedom of relative rotations. In the freely rotating limit (no Boltzmann weight averaging), Salem *et al.* introduced rather complicated multibody interactions in order to obtain a nonzero chiral discrimination. However, their calculated chiral discrimination was very small even at short distances. They also performed a calculation at finite temperature and calculated $U_2(R)$ for the D–D and D–L pairs, assigning partial charges to the four vertices and tracing over the electrostatic interactions. The numerical averaging (integration) did not fully converge for the shorter distances. In all cases their difference in the calculated internal energies was never more than one part in 10^3 of the averaged internal energy.

One of the major ways we increased substantially the chiral discrimination was to introduce an additional asymmetry in the C_α bond lengths (in ref 12, the tetrahedra were all of equal bond length). We find it to enhance quite dramatically the chiral discrimination, and we think that this is a real effect that combines an asymmetry in the molecular shape with asymmetric interactions to produce a large chiral discrimination. Whereas the largest value of the relative internal energy difference found in ref 12 was 10^{-3} (T = 300 K), we found values up to 10^{-1}.

In addition, the number of points used in our five-dimensional integration is up to 10 times larger[25] than in ref 12. This ensured us of good convergence even for the shortest distances. We note that with the Lennard–Jones potentials the convergence was even better than with longer range electrostatic interactions. This is due partially to poor convergence of the electrostatic sums because of canceling effects of positively and negatively charged groups in neutral molecules.

Finally, we do not think that defining the chiral discrimination as the difference in internal energies $U_2^{DD}(R) - U_2^{DL}(R)$ at a given distance R will yield a reliable measure of the overall discrimination. As can be seen in our results, this definition is somewhat ambiguous. The geometrical steric repulsion and the attractive interactions at a larger distance may compete and lead to opposing effects at different intermolecular distances. On the other hand, Δ, as defined in our eq 10 above, averages correctly over the different distances.

(25) Note that the definition of N in in ref 12 is larger than ours by a factor of 2.

V. Chiral Discrimination in Langmuir Monolayers

The results of the previous section can also be applied to the special situation of a chiral molecule with three anchoring points bounded on a two-dimensional plane.[13-14,26] We use here ideas developed by Andelman and de Gennes[13,14] about chiral amphiphiles forming a Langmuir monolayer. Equivalently, this can model physioadsorption on a solid substrate where the molecules have a degree of freedom of lateral diffusing in the plane.[21-23]

Consider a tetrahedron where the only allowed rotations are those where the three groups A, M, and CA are required to stay on a two-dimensional plane (see Figure 6). We can think of this tetrahedron as a tripod amphiphile. The central carbon C_α is attached to three groups that lie at the water/air interface and to a fourth group which is an aliphatic tail pointing away from the interface into the air. This type of molecules can be produced, for example, by replacing the single hydrogen of the alanine by an aliphatic tail.[27] If the tail is long enough, the resulting molecule will form an insoluble monolayer at the water/air interface, namely, a Langmuir monolayer. Since the tail does not contribute to the chiral discrimination (in this special case of tripodal molecules), we do not include its contribution to the intermolecular interactions.

The advantage of studying monolayers is that the geometry is simpler and one might hope to understand better the chiral discrimination. Another advantage is that it is easy to control the surface pressure in a Langmuir trough and to use other techniques like epifluorescence microscopy[28,29] to observed formation of chiral domains.

There are several studies of racemic mixtures of amphiphiles at the water/air interface.[30-38] However, most of the molecules studied are more complicated than a simple tripod (*e.g.*, two

(26) For a general discussion of three-point attachment in biology, see: (a) Bentley, R. *Nature* **1978**, *276*, 673. (b) Bentley, R. *Trans. N. Y. Acad. Sci.* **1983**, *41*, 1.

(27) Wolf, S. G.; Leiserowitz, L.; Lahav, M.; Deutsch, M.; Kjaer, K.; Als-Nielsen, J. *Nature* **1987**, *325*, 63.

(28) (a) Weis, R. M.; McConnell, H. M. *Nature* **1984**, *310*, 47. (b) Weis, R. M.; McConnell, H. M. *J. Phys. Chem.* **1985**, *89*, 4453.

(29) (a) Heckl, W. M.; Möhwald, H. *Ber. Bunsen-Ges. Phys. Chem.* **1986**, *90*, 1159. (b) Heckl, W. M.; Lösche, M.; Cadenhead, D. A.; Möhwald, H. *Biophys. J.* **1986**, *14*, 11.

(30) Zeelen, F. J. Doctoral Thesis, State University of Leiden, The Netherlands, 1956 (unpublished).

(31) (a) Arnett, E. M.; Chao, J.; Kinzig, B. J.; Stewart, M. V.; Thompson, O. *J. Am. Chem. Soc.* **1978**, *100*, 5575. (b) Arnett, E. M.; Chao, J.; Kinzig, B. J.; Stewart, M. V.; Thomspon, O.; Verbiar, R. J. *Ibid.* **1982**, *104*, 389.

Table III. Parameters for the Model Tripodal Molecules Interacting via a Pure Lennard-Jones Potential[a]

group	bond length[b] to C_α	σ [b]	ϵ [c]
C_α	0.0	1.8	-0.1
A	2.25	2.0	-0.35
M	1.5	1.6	-1.5
CA	3.0	3.2	-0.5

[a] Same notation as in Table II. The three groups A, M, and CA sit at the corners of a triangle and the C_α at its center, as is illustrated in Figure 6. [b] Distances in Å. [c] Energies in kJ/mol.

chiral centers). Nevertheless, it is interesting to study rigid tripodal amphiphiles because of their simplicity.

In the two-dimensional geometry, there are only two degrees of freedom describing the relative rotation of one basal plane with respect to the other. We used the Simpson integration method, in a way similar to that explained in the previous section. Here, the number of integration points is $(2N + 1)^2$, and in our calculations, N was varied between $N = 40, 60, 80$, and even 100 in some runs. Convergence was always achieved to better than 10^{-5}. The interaction parameters as well as the various bond lengths are tabulated in Table III.

It is interesting to compare the free energy, internal energy, and entropy for the monolayer (Figure 7) with those of the bulk (Figure 4). The most apparent difference is the deeper minimum in the HOC pair for the free energy in two dimensions (2d's) compared with the three dimension (3d) case. At short distances, the repelling hard core is stronger for HEC than for HOC in both 2d and 3d cases, although in the 3d case the discrepancy is bigger. The entropy is lower for the entire distance range for the HEC case (as in the 3d case), indicating a more frozen state for the HEC. On the other hand, the internal energy U_2 is lower for the HEC (down to distances where the steric hindrance is important) so the combination of the two competing terms in the free energy results in a non-monotonous behavior as a function of the distance.

Most of the differences between the 2d and 3d cases can be understood in terms of the smaller configuration space available in the 2d case. The molecules lock in and repel strongly each other at larger distances in the 2d case. As in 3d's, we think that it is more instructive to look at the integrand $b_2(T,R)R$ (as in eq 8) of the second virial coefficient as a function of the distance R. This is plotted in Figure 8. The two minima in f_2^{DD} and f_2^{DL} manifest themselves in the two peaks of the functions in Figure 8. Integrating the areas under the curves in this figure yields an overall chiral discrimination parameter of $\Delta_{2d} = 0.088$. It is still positive, indicating a preference of the HEC case, but it is not as large as the 3d case where $\Delta_{3d} = 0.43$.

The same conclusion (HEC preference) was reached by Andelman and de Gennes[13-14] for van der Waals interactions in 2d's. However, in their model, only nine discrete rotations (back-to-back) at a fixed intermolecular distance and only the attractive tail of the interaction ($\sim 1/R^6$) have been considered. One of our main findings is again that the chiral preference can strongly depend on the intermolecular distance. In 2d's, especially, we see a strong inversion of the preference (up to about distances of 6.5 Å, it is HOC, whereas above this distance, it is HEC). Finally, it is interesting to note that in 2d's the strong dependence of the chiral preference on distance is caused less by the steric hard core repulsion and more by a different combination of the attractive interactions. Hence, both f_2^{DD} and f_2^{DL} have deep minima at distances around their respective hard core radii.

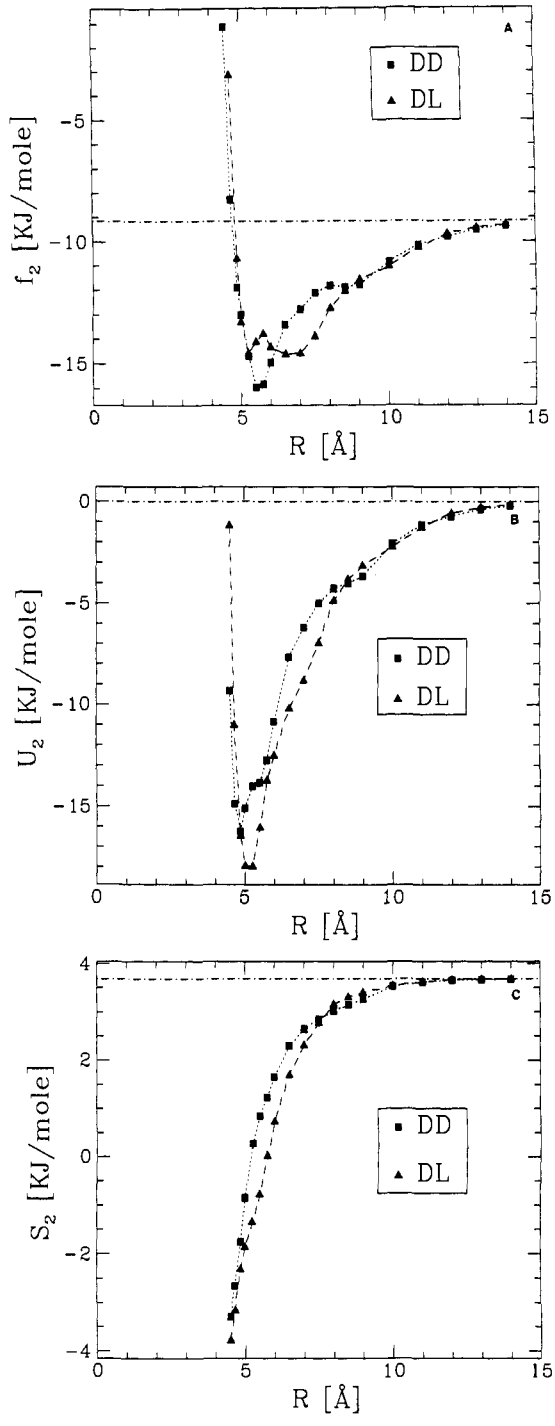

Figure 7. Pair free energy, f_2, internal energy, U_2 and entropy, S_2, in A, B, and C, respectively. Notations are the same as in Figure 4, but the three groups, A, M, and CA, are restricted to lie on a two-dimensional plane as is illustrated in Figure 6. Values of the parameters are given in Table III. The temperature is 300 K. The horizontal dotted-dashed lines denote the values at infinite separation.

VI. Concluding Remarks

In this paper, we have studied the chiral discrimination among molecules possessing a single chiral center. To do so, we have computed the pair free energy, internal energy, and entropy for the two enantiomeric pairs, D–D and D–L, as a function of

(32) For a review on chiral Langmuir monolayers, see *e.g.*: Stewart, V. M.; Arnett, E. M. In *Topics in Stereochemistry*; Allinger, N. L., Eliel, E. L., Wilen, S. H., Eds.; Wiley: New York, 1982.
(33) Wisner, D. A.; Rosario-Jansen, T.; Tsai, M.-D. *J. Am. Chem. Soc.* **1986**, *108*, 8064.
(34) Bouloussa, O.; Dupeyrat, M. *Biochim. Biophys. Acta* **1988**, *938*, 395.
(35) Dvolaitzky, M.; Guedeau, M. A. *Langmuir* **1989**, *5*, 1200.
(36) (a) Arnett, E. M.; Harvey, N. G.; Rose, P. L. *Langmuir* **1988**, *4*, 1049; (b) *Acc. Chem. Res.* **1989**, *22*, 131.
(37) (a) Harvey, N. G.; Rose, P. L.; Mirajovsky, D.; Arnett, E. M. *J. Am. Chem. Soc.* **1990**, *112*, 3547. (b) Heath, J. G.; Arnett, E. M. *J. Am. Chem. Soc.* **1992**, *114*, 4500.
(38) Stine, K. J.; Uang, J. Y.-J.; Dingman, S. D. *J. Am. Chem. Soc.*, in press.

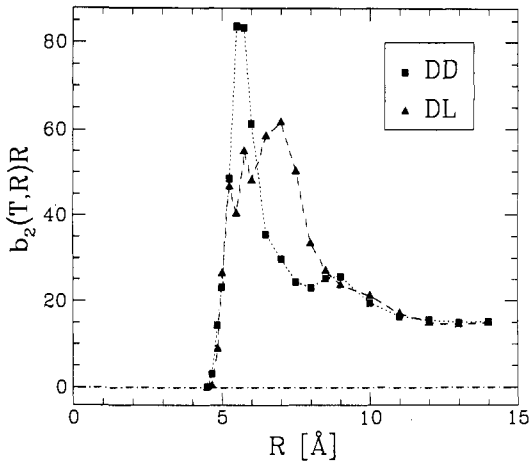

Figure 8. Integrand of the second virial coefficient, $b_2(T,R)R$ in 2D, as a function of the inter-pair distance R. Notations are the same as in Figure 5. This is the adapted second virial coefficient for *tripodal* molecules restricted to rotate in the plane. The chiral discrimination, Δ, is proportional to the difference in the areas under the two curves. Like the three-dimension case (Figure 5), in two dimensions the D–L pairs are preferred energetically (HEC).

intermolecular distance. Then, we deduced the second virial coefficient for the homo- and heterochiral cases. Our definition of the chiral discrimination in terms of the second virial coefficient is motivated by the fact that this second virial coefficient enters in the low density expansion of the equation of state of the mixture.

We used a Monte Carlo simulation method to resolve the chiral discrimination in alanine molecules with realistic (CHARMM) potentials. Although we used very long computer runs, the discrimination turned out to be too small to be computed and lies within the stochastic errors of the simulations. We observed only a very small discrimination (especially at lower temperatures), and for short distances.

On the other hand, we have been able to obtain large chiral discriminations for model molecules with sufficiently strong asymmetry. This discrimination is obtained with standard two-body interactions in both two and three dimensions, and at a finite temperature, in contrast with previous calculations.[12]

One of our main results can be seen in the discrimination of the model molecules (Figures 4–8). The free energy (or internal energy) difference between D–D and D–L molecules as a function of the distance of their centers *changes signs* in some cases. The homochiral case is favored at shorter distances, whereas the heterochiral case is favored at larger distances. Simple rules like the Wallach's rule[39] about the relative stability of racemic compounds as compared with their pure enantiomeric counterparts should be considered with great care.[9,40] As we have shown in this paper, the chiral discrimination does not have only a geometrical origin (close packing) but stems also from other, longer range interactions, leading to a more complicated picture.

Our findings relying on the so-defined chiral discrimination are relevant for problems where chiral discrimination is considered in fluid phases (liquid or gas) of racemic mixtures; such is the case, for example, of experiments using techniques like gas chromotography to find discrimination between dimers of D and L enantiomers. Yet another relevant case is chiral discrimination in racemic liquid mixtures, and especially in solutions where the solvent molecules enter between the D–D and D–L pairs so that the discrimination depends on averaging between all possible inter-pair distances.[9,14,20] However, using only the second virial coefficient is, probably, not sufficient in the problem of solidification of racemic mixtures. Whether the mixture will solidify into a racemate or a conglomerate is not governed by low density effects. Rather, it involves virial coefficients of higher order.

In order to study the phase diagram of the mixture in a more systematic way, it seems that the most convenient method would be molecular dynamics or Monte Carlo calculations for an ensemble of D and L enantiomers. One could then make an extensive study of the phase diagram of the mixture as a function of x (the mole fraction of the D enantiomer) and T. Such a study is currently in progress.

Finally, let us note that it would also be interesting to undertake such extended studies for realistic models of more complicated chiral molecules. Indeed, although the two-body effect might again be small, it might still be sufficient to trigger a strongly collective effect such as a phase transition (phase separation, etc.).

Acknowledgment. We would like to thank R. Elber, H. Kagan, M. Lahav, and A. Revcolevschi for useful discussions and correspondence. H.O. would like to thank Tel Aviv University for its hospitality and the Sackler Institute for Solid State Physics for providing a travel grant. D.A. thanks the Service de Physique Théorique, Saclay, for its hospitality and acknowledges partial support from the Israel Academy of Sciences and Humanities and from the German-Israel Binational Foundation (GIF) under Grant No. I-0197.

(39) Wallach, O. *Liebigs Ann. Chem.* **1895**, *286*, 90.
(40) For a recent critical review of the Wallach's rule, see: Brock, C. P.; Schweizer, W. B.; Dunitz, J. D. *J. Am. Chem. Soc.* **1991**, *113*, 9811 and references therein.